

Improved Hybrid Blind PAPR Reduction Algorithm for OFDM Systems

Kwame S Ibwe

College of Information and Communication Technologies, University of Dar es Salaam

P. O. Box 33335, Dar es Salaam, Tanzania

Corresponding author e-mail and telephone number: kwame.ibwe@gmail.com

Abstract

The ever growing demand for high data rate communication services has resulted into the development of long-term evolution (LTE) technology. LTE uses orthogonal frequency division multiplexing (OFDM) as a transmission technology in its PHY layer for down-link (DL) communications. OFDM is spectrally efficient multicarrier modulation technique ideal for high data transmissions over highly time and frequency varying channels. However, the transmitted signal in OFDM can have high peak values in the time domain due to inverse fast Fourier transform (IFFT) operation. This creates high peak-to-average power ratio (PAPR) when compared to single carrier systems. PAPR drives the power amplifiers to saturation degrading its efficiency by consuming more power. In this paper a hybrid blind PAPR reduction algorithm for OFDM systems is proposed, which is a combination of distortion technique (Clipping) and distortionless technique (DFT spreading). The DFT spreading is done prior to clipping reducing significantly the probability of having higher peaks in the composite signal prior to transmission. Simulation results show that the proposed algorithm outperforms unprocessed conventional OFDM transmission by 9 dB. Comparison with existing blind algorithms shows 7 dB improvement at error rate 10^{-3} and 3 dB improvement at error rate 10^{-1} when operating in flat fading and doubly dispersive channels, respectively.

Keywords: LTE Systems, OFDM, Peak to Average Power Ratio, DFT spreading, Signal to Noise Power Ratio

Introduction

The advancement in wireless communication technologies has led to massive deployment of portable battery powered hand-held devices, data-hungry applications and services. To accommodate these, energy and spectral efficient communication systems are needed. The third generation partnership project (3GPP) launched long-term evolution (LTE) to achieve high spectral and data throughput efficiency (Sriharsha et al. 2017). LTE released 8 achieves theoretical data rates for downlink (DL) and uplink (UL) of up to 100 Mbps and 50 Mbps, respectively (Cox 2014). Orthogonal frequency division multiplexing (OFDM) is used in DL because of its ability to suppress frequency and time selectivity of

the channel (Chiavaccini and Vitetta 2000). However, the transmitted signal in OFDM system can have high peak values in the time domain when subcarrier components are added via an inverse fast Fourier transformation (IFFT) operation (Davis and Jedwab 1997). These large peaks drive the power amplifiers of the devices to saturation (Saeedi et al. 2002). Hence, mitigation of high PAPR problem in OFDM systems is important in order to achieve energy efficiency for the limited battery powered devices, better spectrum utilization and optimum system performance.

Thompson (2005) proposed design of systems with very high signal peaks in order to avoid clipping. However, this approach leads to very high power consumption (since

the power amplifier must have high supply rails) which is not practical for battery powered devices. The authors in Han and Lee (2005) suggest applying digital signal processing that reduces such high peak values in the transmitted signal thus avoiding clipping. These methods are commonly referred to as peak-average ratio (PAR) reduction. PAR reduction methods are categorized into transmitter enhanced techniques, receiver enhanced techniques and signal transformation techniques (Joo et al. 2010, Liu et al. 2018). The PAPR reduction schemes can be further divided into distortionless and non-distortionless techniques. Distortionless techniques include coding (Davis and Jedwab 1997), tone reservation (Han and Lee 2005), trellis-shaping (Litsyn 2007), and multiple signal representation (aka selected mapping (SLM)) (Li and Cimini 1998) or partial transmit sequences (PTS) constellation extension (Joo et al. 2010). Non-distortionless schemes include peak cancellation (Van Nee and De Wald 1998) and signal clipping (Saedi et al. 2002, Cheng et al. 2017, Mounir et al. 2017). The second category, receiver enhanced techniques, have been suggested in Wang et al. (1999) (maximum-likelihood decoding) and in Myung et al. (2006), signal reconstruction. The third category includes constant envelope OFDM which uses a phase modulator as the transformer (Thompson 2005, Ann and Jose 2016). Distortion techniques do not require any side information to be sent to the receiver and they have low complexity compared to the distortionless techniques. However, the distortion techniques are considered to introduce spectral re-growth which increases the error rate of the system. Distortionless techniques require sending side information to the receiver to mitigate the PAPR problem. Sending of side information degrades the spectral efficiency by consuming bandwidth sending non-user data (Joo et al. 2010, Fanggang and Xiaodong 2011).

Shafter and Rao (2016) used continuous phase modulation (CPM) with repeated clipping and frequency domain filtering to reduce PAPR. However, this method brings high implementation complexity for an optimal receiver and the repeated clipping degrades the error rate performance. In reference, Offiong et al. (2017) proposed a novel characterization of pilot-assisted (PA) method for PAPR reduction in optical OFDM systems. This method uses side information for the signal shaping at the receiver side. The authors in Ikpehai et al. (2017) proposed energy efficient method for PAPR reduction in power line systems. This method focuses on the linearization of the HPA by suppressing the impulsive noise. But detailed noise characteristics of the system cannot be known before transmission. Hence, this method has limitation and cannot be extended to wireless or optical OFDM systems. Yoshizawa and Ochiai (2017) proposed a trellis-assisted constellation subset method for PAPR reduction. The major challenge in this method is on the choosing of the subset from the original constellation phasers.

This paper presents a theoretical characterization of the OFDM transmit signal for PAPR reduction in wireless OFDM using hybrid blind techniques. Blind techniques used do not rely on side information but the statistics of the OFDM transmitted signal only. The presented method is a combination of distortion and distortionless techniques. These are clipping and discrete Fourier transform (DFT) spread. The DFT spreading is done prior to clipping; this reduces significantly the probability of having higher peaks in the composite signal prior to transmission on HPA after which clipping proceeds to take care of the remaining possible higher peaks. The contributions of this paper include analysis of the transmit signal format prior to HPA transmission. The analysis elaborates the key parameters to be configured when implementing the system onto hardware. The detailed pseudocode on the implementation of proposed algorithm is

given. The PAPR reduction is characterized by considering the cumulative distribution function (CCDF) metric in accordance with the general way of presenting results on the subject (Ann and Jose 2016). Detailed mathematical analysis is given to show the exponential increase of PAPR with the number of subcarriers. A comparison of existing algorithms is done, to obtain the PAPR reduction capability in error rate performance. The error rate performance is assessed in terms of bit mean squared error to noise power ratio. These results are obtained using simulation platform, MATLAB®. To test for the performance of the hybrid transmit signal AWGN and double dispersive wireless channel environments are used. The channel models used are from Proakis (2001) and Chiavaccini and Vitetta (2000) for AWGN and double dispersive channel, respectively.

Materials and Methods

OFDM signal

In an OFDM system a frequency bandwidth B is divided into N non-overlapping orthogonal subcarriers of bandwidth Δf ; where $B = N\Delta f$. For a given OFDM symbol, each subcarrier is modulated with a complex value taken from a known constellation (e.g., QAM, PSK, etc.). Let us denote a block of N frequency domain subcarriers as a vector $\mathbf{X} = [X_0, X_1, \dots, X_{N-1}]$. In the time domain, via an IFFT operation we obtain $\mathbf{x} = [x_1, x_2, \dots, x_{N-1}]$. Thus, the sampled sequence at the transmitter is given as:

$$x[n] = \frac{1}{\sqrt{N}} \sum_{k=0}^{N-1} X_k e^{j2\pi kn/N} \quad 1$$

where $\{X[k]\}$ are QPSK modulated data symbols. It is observed that, $x[n]$ is obtained by adding N different time-domain orthogonal

signals $\left\{ e^{j2\pi kn/N} \right\}$ each modulated with data

symbol $X[k]$. Figure 1 shows the sum of time-domain In-phase and Quadrature QPSK-

modulated subcarrier signals $X[k]e^{j2\pi kn/N}$ for $N=8$. The PAPR characteristics of the OFDM signal is obvious from Figure 1 and it is expected to increase as N increases.

PAPR definition

The PAPR is a figure of merit which describes the dynamic range of the OFDM time domain signal. The continuous time domain OFDM signal at time index n is given as;

$$x_n(t) = \frac{1}{\sqrt{N}} \sum_{k=0}^{N-1} X_{n,k} g_k(t - nT) \quad 2$$

where $T = \frac{1}{\Delta f}$ and g_k is the rectangular

pulse shaping filter defined as;

$$g_k(t) = \begin{cases} e^{j2\pi k\Delta f t} & 0 \leq t < T \\ 0 & \text{else} \end{cases} \quad 3$$

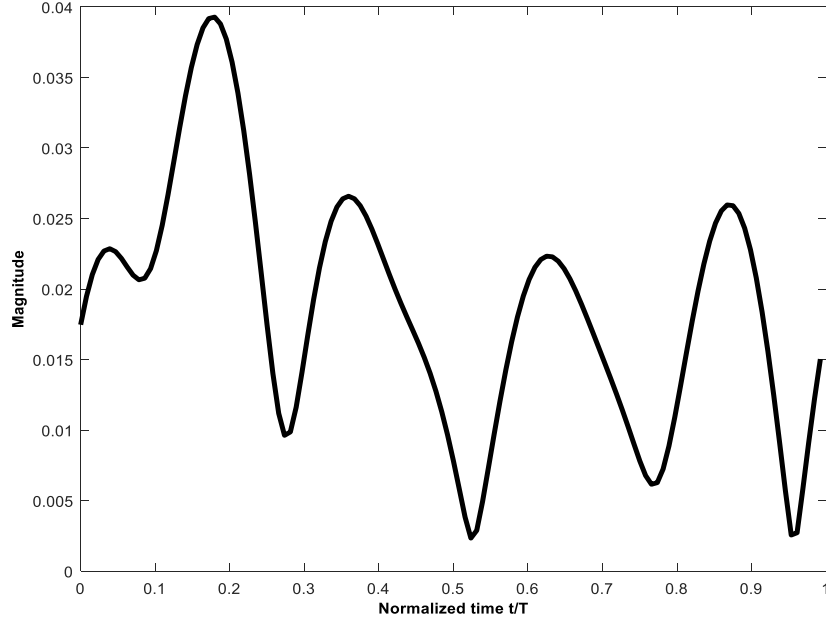


Figure 1: Magnitude of the signal in equation 1.

From equation 2 the Root Mean Square (RMS) magnitude of the OFDM signal is defined as the root of the time average of the envelope power ($\sqrt{\bar{P}}$), where \bar{P} is defined as;

$$\bar{P} = \frac{1}{T} \int_{t=0}^T |x(t)|^2 dt = \frac{1}{N} \sum_{k=0}^{N-1} |X_{n,k}|^2 \quad 4$$

The value of \bar{P} in this case corresponds to a single OFDM symbol and depends on the sequence of information carrying coefficients $\{X_{n,k}\}$. The average power of OFDM symbols can be written as $P_{av} = E\{\bar{P}\}$. Thus, the conventional definition of the PAPR for the OFDM symbol in the continuous time domain may be expressed as;

$$PAPR(x(t)) = \frac{\max_{t \in [0, T]} |x(t)|^2}{E\{|x(t)|^2\}} \quad 5$$

If the input data power is normalized, then $E\{|x(t)|^2\} = 1$, and equation 5 results into

$$PAPR(x(t)) = \max_{t \in [0, T]} |x(t)|^2 \quad 6$$

$$\begin{aligned} &= \max_{t \in [0, T]} \left| \frac{1}{\sqrt{N}} \sum_{k=0}^{N-1} X_k e^{j2\pi k \Delta f t} \right|^2 \\ &\leq \frac{1}{N} \left| \sum_{k=0}^{N-1} X_k e^{j2\pi k \Delta f t} \right|^2 \\ PAPR(x(t)) &\leq N \quad 7 \end{aligned}$$

The expression in equation 7 validates the hypothesis that maximum PAPR is equal to the number of subcarriers N. The PAPR for the discrete-time baseband signal $x[n]$ may

not be the same as that for the continuous-time baseband signal $x(t)$. It is known that $x[n]$ can have almost the same PAPR as $x(t)$ if it is L-times interpolated (oversampled) (Saeedi et al. 2002). Signal $x[n]$ can be expressed in terms of the L-times interpolated version as;

$$x'(n) = \frac{1}{\sqrt{LN}} \sum_{k=0}^{LN-1} X'[k] e^{j2\pi\Delta fkn} \quad 8$$

with

$$X'[k] = \begin{cases} X[k], & \text{for } 0 \leq k < \frac{N}{2} \text{ and } NL - \frac{N}{2} < k < NL \\ 0, & \text{otherwise} \end{cases}$$

where $\Delta f = \frac{1}{T}$ (the subcarrier spacing). For such an L-times interpolated signal, the PAPR is now redefined as;

$$PAPR(x'[n]) = \frac{\max_{n=0,1,\dots,NL} |x'[n]|^2}{E\{|x'[n]|^2\}} \quad 9$$

where $E\{\cdot\}$ denotes the expectation operation. PAPR increases exponentially with number of subcarriers. Reducing $\max |x'[n]|$ is the principle goal of PAPR reduction in OFDM systems to achieve 0 dB transmissions. This is usually tested by finding the probability that the signal power is out of the linear range of the HPA. Taking $\{Z_n\}$ to be magnitudes of

complex samples $\left\{x\left[\frac{nT_s}{N}\right]\right\}_{n=0}^{N-1}$, and

assuming that average power is equal to one, $E\{x(t)^2\} = 1$, then $\{Z_n\}$ are independent and identically distributed Rayleigh random variables normalized with its own power, with the following probability density function:

$$f_{Z_n}(z) = \frac{z}{\sigma^2} e^{-\frac{z^2}{2\sigma^2}} = 2ze^{-z^2}, \quad 10$$

$n = 0, 1, 2, \dots, N - 1$

where $E\{Z_n^2\} = 2\sigma^2 = 1$. It is noted that crest factor (CF), $CF = \sqrt{PAPR}$ is equivalent to maximum of Z_n . The cumulative distribution function (CDF) of Z_{\max} is given as

$$F_{Z_{\max}}(z) = P(Z_{\max} < z) = P(Z_0 < z) \cdot P(Z_1 < z) \dots P(Z_{N-1} < z) \quad 11$$

$$= (1 - e^{-z^2})^N$$

where

$$P(Z_n < z) = \int_0^z f_{Z_n}(x) dx, \quad n = 0, 1, 2, \dots, N - 1.$$

To find the probability that Z_{\max} exceeds z , complementary CDF (CCDF) is used and defined as

$$\begin{aligned} \tilde{F}_{Z_{\max}}(z) &= P(Z_{\max} > z) \quad 12 \\ &= 1 - P(Z_{\max} \leq z) = 1 - F_{Z_{\max}}(z) \\ &= 1 - (1 - e^{-z^2})^N \end{aligned}$$

The derivations of equation 11 and equation 12 are made under the assumptions that OFDM signal samples N are independent and N is sufficiently large. But equation 11 and equation 12 do not hold for bandlimited and oversampled signals due to the fact that sampled signals do not necessarily contain the maximum point of the original continuous-time signal. Hence, simplified test for PAPR uses CCDF approximated as

$$\tilde{F}_{Z_{\max}}(z) = (1 - e^{-z^2})^{\alpha N} \quad 13$$

where α is determined by fitting the theoretical CDF into the actual one. Experiments in (Van Nee and De Wild 1998) have shown that $\alpha = 2.8$ is appropriate for large values of N. Equation 13 is the analytical distribution of PAPR of unprocessed OFDM signal in equation 2.

DFT spreading

The DFT-spreading technique uses the concept of orthogonal frequency division multiple access (OFDMA) (Cox 2014). The spreading is achieved when the outputs of M-

point DFT are spread across the N-point IDFT for $N > M$. The DFT (FFT) and IDFT (IFFT) operations usually cancel each other making the OFDMA system equivalent to single carrier FDMA (SC-OFDMA). In this sense the PAPR of the SC-FDMA system will theoretically be equal to single carrier system.

To remove the uncertainty of having any PAPR in the output signal, it is proposed that hybrid model of the transmitter is designed by incorporating clipping after DFT-spreading. The block diagram of the proposed model is shown in Figure 2.

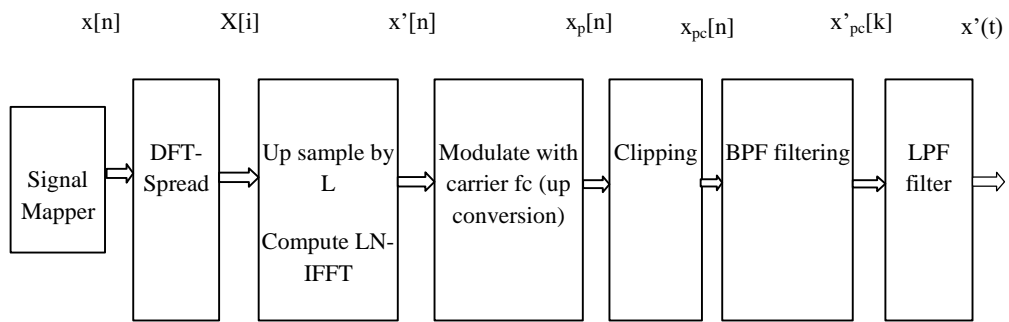


Figure 2: The model of the proposed hybrid blind algorithm.

Figure 3 shows two ways of spreading the M-point DFT outputs into the N-point IFFT processor. DFDMA (Distributed FDMA) and LFDMA (Localized FDMA). The DFDMA distributes M-DFT outputs over the entire band (of total N subcarriers) with zeros filled in (N-M) unused subcarriers, whereas LFDMA allocates DFT outputs to M consecutive subcarriers in N subcarriers. When DFDMA distributes DFT outputs with equidistance $N/M = S$, it is referred to as IFDMA (Interleaved FDMA) where S is called the bandwidth spreading factor. The

main goal is to transmit the 0 dB PAPR output signal $x'(t)$ to the receiver. This is achieved by first M-point DFT spreading the mapped (modulated) data symbols onto N-point IFFT subcarriers, up sampled by a factor L, passed through LN-point IFFT processor, modulated by a carrier frequency f_c and then clipping the output signal $x_{pc}[n]$ so as the transmitted signal $x'(t)$ is guaranteed 0 dB PAPR.

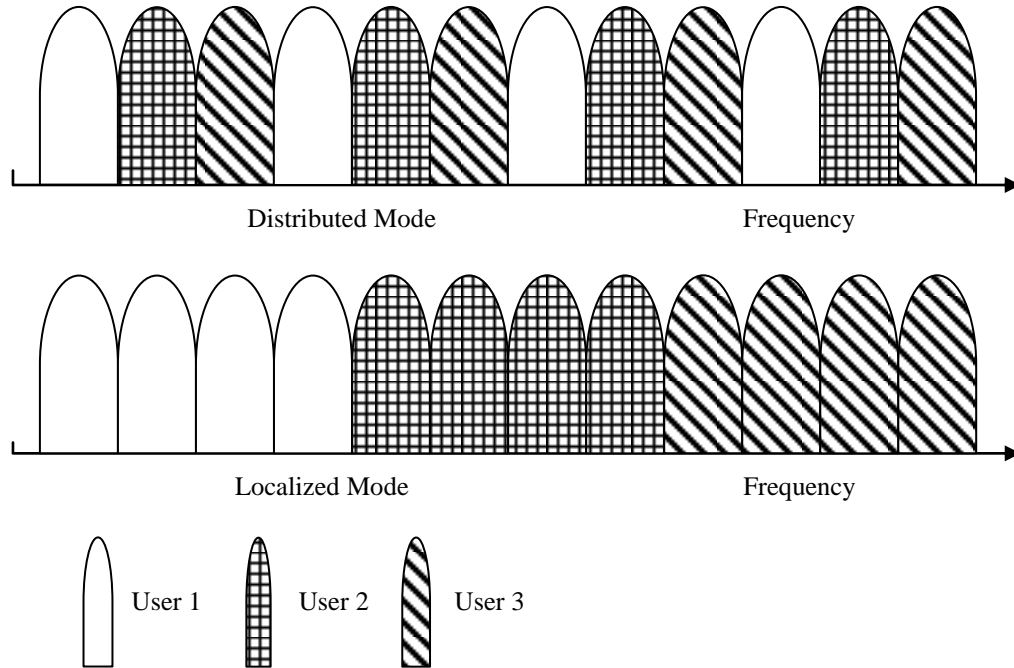


Figure 3: Subcarriers allocation to multiple users according to DFDMA and IFDMA for $N = 12$, $M = 4$ and $S = 3$.

For IFDMA the generated M -point DFT-spread sequence $X[i]$ are obtained from input modulated data sequence $x[n]$ as;

$$\tilde{X}[k] = \begin{cases} X\left[\frac{k}{s}\right], \\ 0, \text{ otherwise} \end{cases} \quad 14$$

$$k = S \cdot m, \quad m = 0, 1, \dots, M - 1$$

The DFT-spread sequence $\tilde{X}[k]$ is then up sampled by a factor $L \geq 4$, and then fed into LN IFFT processor. The output of the LN -point IFFT processor is then given as;

$$x'[n] = x'[Lm + s], \quad 15$$

$$s = 0, 1, 2, \dots, S - 1; \quad m = 0, 1, 2, \dots, M - 1$$

$$x'[n] = \frac{1}{LN} \sum_{k=0}^{LN-1} X'[k] e^{j2\pi \frac{k}{LN} n} \quad 16$$

$$x'[n] = \frac{1}{LS} \cdot x[m] \quad 17$$

It is observed in equation 17 that the IFFT output signal $x'[n]$ is equal to the original signal scaled by $\frac{1}{LS}$ in time domain. For LFDMA scheme, the IFFT input signal $X'[k]$ is given as;

$$X'[k] = \begin{cases} X\left[\frac{k}{L}\right], & k = 0, 1, 2, \dots, LM - 1 \\ 0, & k = LM, LM + 1, \dots, LN - 1 \end{cases} \quad 18$$

The IFFT output sequence will be given as;

$$x'[n] = x'[Lm + s] = \frac{1}{LN} \sum_{k=0}^{LN-1} X'[k] e^{j2\pi \frac{k}{LN} n} \quad 19$$

For $s = 0$, equation 19 reduces to equation 17. But for $s \neq 0$, it reduces to;

$$x'[n] = \frac{1}{LS} e^{j\pi \frac{(M-1)s - LSm}{LSM} n} \cdot \beta(m, s, l) \cdot \hat{x}(l) \quad 20$$

where

$$\beta(m, s, l) = \sum_{l=0}^{M-1} \frac{\sin\left(\pi \frac{s}{LS}\right)}{M \cdot \sin\left(\pi \frac{LSm+s}{LSM} - \pi \frac{l}{M}\right)}$$

and $\hat{x}(l) = e^{j\pi \frac{l}{M}} \cdot x[l]$

It is observed from equation 20 that the time domain LFDMA signal becomes the 1/LS scaled copies of the input sequence at the multiples of LS in time domain. The values in between are obtained by summing all the input sequences with different complex-weight factors.

Clipping

Signals in equations 19 and 20 are fed into HPA for modulation with carrier frequency f_c to yield a discrete pass band signal $x_p[n]$ as

$$x_p[n] = \text{Re}\{x'[n] \cdot e^{j2\pi f_c n}\} \quad 21$$

Assuming that upper frequency $f_c + \frac{B}{2}$ is a multiple of the bandwidth B i.e., $f_c + \frac{B}{2} = kB$ where k is a positive integer, equation 21 reduces to equation 22. For even values of n , i.e. $n = 2m$, it reduces to equation 23.

$$x_p[n] = x'[n] \cos \frac{\pi n(2k-1)}{2} \quad 22$$

$$x_p[2m] \equiv x'[m] \cos \pi m(2k-1) = (-1)^m x'(m) \quad 23$$

Then, $x_p[n]$ will be clipped prior to transmission yielding $x_{pc}[n]$. The clipped signal is expressed as;

$$x_{pc}[n] = \begin{cases} x_p[n] & \text{if } |x_p[n]| < A \\ \frac{x_p[n]}{|x_p[n]|} \cdot A & \text{otherwise} \end{cases} \quad 24$$

where A is the pre-specified clipping level. Clipping ratio (CR) is defined as clipping

level normalized by the root mean square (RMS) value σ of the OFDM signal, such that $CR = \frac{A}{\sigma}$. The discrete time bandpass filtered signal $x'_{pc}[n]$ is then transformed to continuous time signal $x'(t)$ by a low pass filter. Using largest order statistics (Papoulis and Pillai 2002), the PDF of the amplitude of the clipped transmitted signal $x'[t]$ is given as;

$$f_{Z_{\max}}(z) = \frac{1}{LS} f_{Z_n}(z) \cdot \left[\int_0^z f_{Z_n}(t) dt \right]^{N-M} \quad 25$$

$$= \frac{d[F_Z(z)^N]}{dz}$$

From equation 25, the PDF of one transmitted OFDM symbol is given as

$$f_Z(z) = \frac{1}{LS} \left(\int_0^z f_{Z_{\max}}(t) dt \right)^{1/N-M} \cdot f_{Z_{\max}}(z) \quad 26$$

$$= \frac{1}{LS} \cdot f_Z(z) \cdot (1 - [1 - Y(z)^N])^{1/N-M} \cdot Y(z)^{N-M} \cdot (1 - Y(z)^N)$$

where $Y(z) = 1 - e^{-z^2}$. Hence, the CCDF of the processed LFDMA OFDM signal is evaluated from equations 20 and 25 as;

$$F_{Z_{pnc}}(z) = 1 - (1 - 2Q(\sqrt{z}))^{\alpha(N-M)} \quad 27$$

where $Q(x) = \frac{1}{2\pi} \int_x^\infty e^{-u^2/2} du$ represents the Q-

function and α is an empirical factor defined in equation 13. Equation 27 is based on the assumption that the IFFT output samples approach Gaussian random variables as N increases. For IFDMA OFDM processed signal, equation 17 is the input to the HPA prior to clipping. Hence, the CCDF of the IFDMA processed transmitted OFDM signal is given as;

$$F_{Z_{pnc_IFDMA}}(z) = 1 - (1 - 2Q(\sqrt{z}))^{\frac{\alpha(N-M-1)}{LS}} \quad 28$$

To estimate the error rate performance of the proposed system, the PAPR threshold for clipping λ is defined as $\lambda \cong \frac{A}{P_{in}}$, where the

input power $P_{in} = \int_0^{\infty} z^2 f_Z(z) dz$ and A is the maximum permissible amplitude defined in equation 24. Then, the total output power after clipping is obtained as;

$$P_{out} = \int_0^A z^2 f_Z(z) dz + \int_A^{\infty} A^2 f_Z(z) dz \quad 29$$

and the total distortion rate χ is given as

$$\chi = \frac{\left(\int_0^A z^2 f_Z(z) dz + \int_A^{\infty} A \cdot z \cdot f_Z(z) dz \right)}{P_{in}} \quad 30$$

Estimating the total attenuation factor,

$$K = \frac{\chi^2 P_{in}}{P_{out}},$$

the signal to noise plus interference ratio (SNIR) is given as;

$$SNIR = \frac{K \cdot \frac{E_s}{N_0}}{(1-K) \frac{E_s}{N_0} + 1} \quad 31$$

where $\frac{E_s}{N_0}$ is the signal to noise power ratio.

The bit error rate (BER) performance of the system over AWGN channel for QPSK

modulated signal is given as $P_B = Q(\sqrt{SNIR})$. Furthermore, QPSK symbol error rates simply follows as: $P_S = 1 - (1 - P_B)^2$. Under frequency selective channels (Proakis 2001), the BER is given by

$$P_B = \int_0^{\infty} Q \left(\frac{\sqrt{\kappa^2 \cdot K \cdot \frac{E_s}{N_0}}}{\sqrt{\kappa^2 \cdot (1-K) \frac{E_s}{N_0} + 1}} \right) f_Z(\kappa) d\kappa \quad 32$$

where κ is the channel attenuation which is Rayleigh distributed with $E[\kappa^2] = 1$.

Proposed Algorithm

The discussion on DFT spreading and clipping techniques has led to the formulation of a hybrid blind PAPR reduction algorithm. This algorithm does not require side information to assist reduction process, rather depend only on the signal structure after DFT spread and clipping to reduce PAPR for linear HPA transmission. The proposed algorithm is given in Table 1.

Table 1: Hybrid blind PAPR reduction algorithm

Step	Action
i.	Set the values of S , M and N .
ii.	Compute the M -point DFT, $X[i]$, of the input data sequence $x[n]$.
iii.	Spread the M -point DFT outputs, $[i]$, onto N -subcarriers of the N -point IFFT processor using either IFDMA or LFDMA to yield $X[k]$.
iv.	Upsample the spread samples $X[k]$ by a factor of L and then compute LN -point IFFT to yield $\acute{x}[n]$.
v.	Modulate the $\acute{x}[n]$ with carrier frequency f_c and clip the passband signal $x_p[n]$ to yield $x_{pc}[n]$.
vi.	Bandpass filter the clipped signal to remove the out of band radiation.
vii.	Convert the bandpass filtered discrete time signal $\tilde{x}_{pc}[n]$ to continuous time signal $\tilde{x}(t)$ for transmission.

Results and Discussion

The complementary cumulative distribution function (CCDF) of the PAPR is the most used performance measure for PAPR reduction techniques. To test for the

performance of the proposed method, parameters specified in Table 2 are used with 10^7 randomly generated symbols.

Table 2: Parameters used for simulating proposed hybrid algorithm

Parameter	Value
Bandwidth	1 MHz
Oversampling factor, L	8
Sampling frequency, f_s	8 MHz
Carrier frequency, f_c	2 MHz
FFT – size, N	256
DFT – size, M	64
Spread bandwidth, S	4
Clipping ratio (CR)	0.8, 1.0, 1.2, 1.4, 1.6
Cyclic prefix, G	64
Modulation order	4/16/64 – QAM

AWGN channel conditions specified in Proakis (2001). The accuracy of the derived analytical expressions for CCDF of PAPR from equations 13, 27 and 28 are verified and compared with simulations results. Results show a good agreement between analytical and simulated results for OFDMA, LFDMA and IFDMA. There is, however, a difference in PAPR levels of about 0.1 dB between analysis and simulation. This is because the analysis assumes perfect Gaussian distribution of the OFDM signal, while simulation only considers Gaussianity as N increases. Both IFDMA and LFDMA outperform OFDMA by at least 9 dB. It is further seen in Figure 4 that IFDMA performs better than LFDMA by 3 dB because IFDMA exploits more frequency diversity.

Figure 4 shows the CCDF plot of unprocessed and processed QPSK OFDM signals at a fixed clipping ratio of 1.2 under

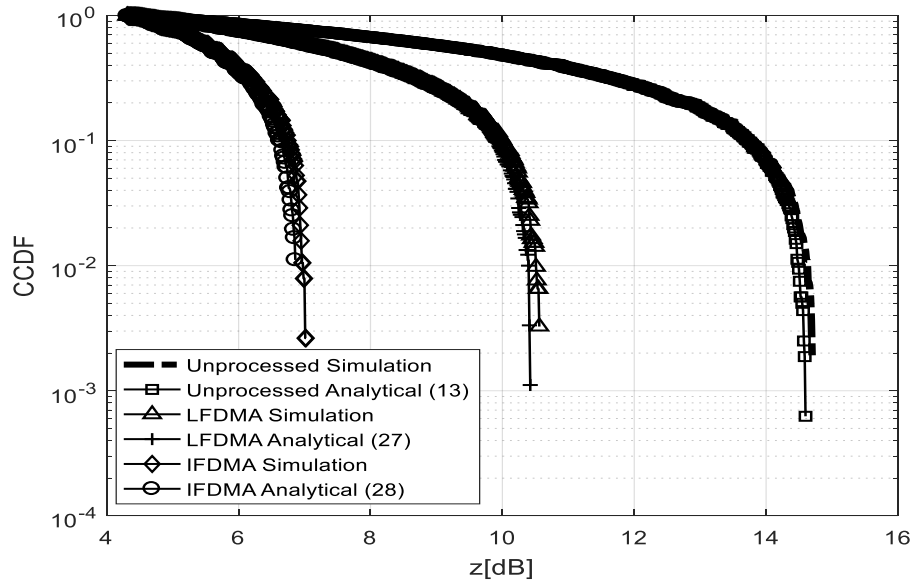


Figure 4: PAPR distribution of analytic and simulated unprocessed, LFDMA and IFDMA signal at CR of 1.2.

Figure 5 represents IFDMA performance at different clip ratios under AWGN channel. It is observed that the PAPR of the OFDM signal decreases significantly by 9 dB after being processed by the proposed algorithm. It is observed in Figures 6 and 7 that the PAPR

performance of the proposed algorithm varies depending on the subcarrier allocation method used under AWGN channel. Comparing the CCDF of OFDMA, LFDMA and IFDMA the results show a meager difference between results obtained via simulation and those of

the theoretical expressions 13, 27 and 28 for chosen symbol modulations. As the higher modulation orders are used more transmit power is needed, hence, accounting for reduced PAPR reduction gain as modulation order increases. For the case of 16-QAM, the values of PAPR with IFDMA, LFDMA and OFDMA (no spreading) for CCDF of 1% are 3.5 dB, 7.2 dB and 9.4 dB, respectively. It implies that the PAPRs of IFDMA and LFDMA are lower by 6.8 dB and 3.7 dB, respectively, than that of OFDMA with no hybrid processing. For all the cases discussed, traditional rectangular filter has been used for pulse shaping after IFFT.

Figure 8 compares the PAPR distribution of the proposed algorithm with the work done by Liu et al. (2018) under AWGN channel. Liu et al. (2018) proposed the use of multicarrier faster than nyquist (MFTN)

signals for nonlinear satellite communication systems. Close agreement is observed for proposed and Liu et al. (2018) distributions. The proposed IFDMA is outperformed by 0.4 dB due to time and frequency diversity gain in Liu et al. (2018) method. In Figure 9 the effect of pulse shaping is examined at fixed CR of 1.2. It is observed that PAPR performance using IFDMA can be substantially improved by increasing the roll off factor from $\alpha = 0$ to 1. But for LFDMA the effect is not significant. Hence, the optimal transmission parameters have to be determined since IFDMA have a trade-off between excess bandwidth and PAPR performance. The effect of varying the number of subcarriers, M , used in spreading is studied in Figure 10. It is observed that PAPR degrades as M increases.

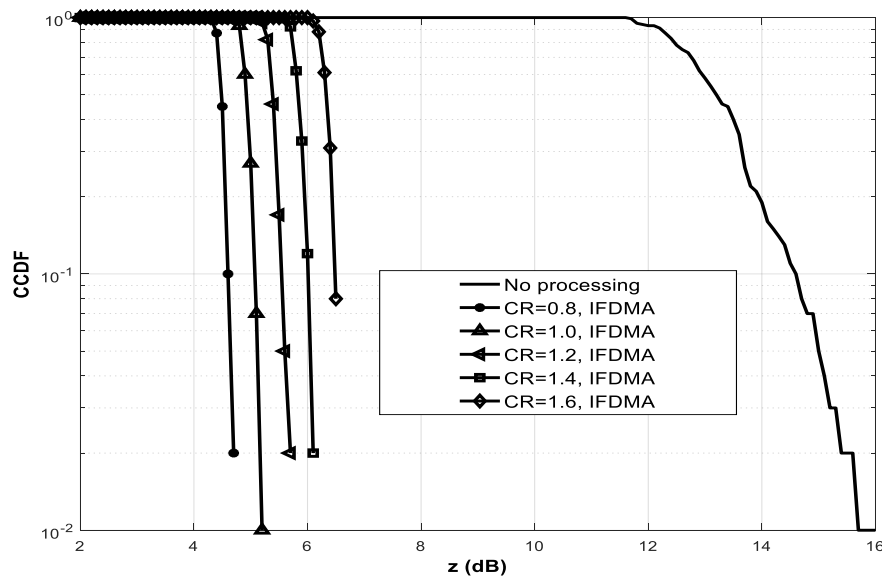


Figure 5: PAPR distribution for IFDMA and unprocessed OFDM for different clipping ratios.

In Figure 11 the performance of the proposed algorithm is compared with existing methods presented in (Shafter and Rao 2016) and Liu et al. (2018) under AWGN channel.

To test for channel performance, minimum square error (MSE) of the received symbols is used as a standard metric.

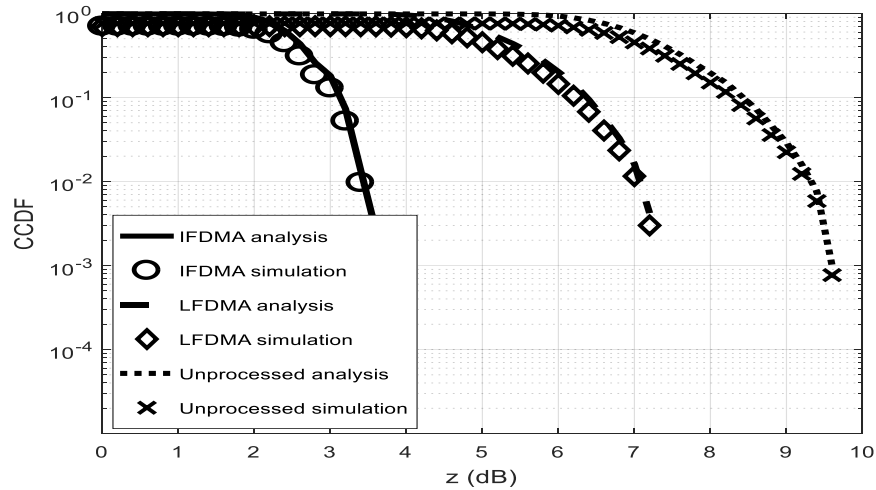


Figure 6: PAPR distribution of analytic and simulated OFDMA, IFDMA and LFDMA at CR = 1.2 with 16 QAM modulated symbols.

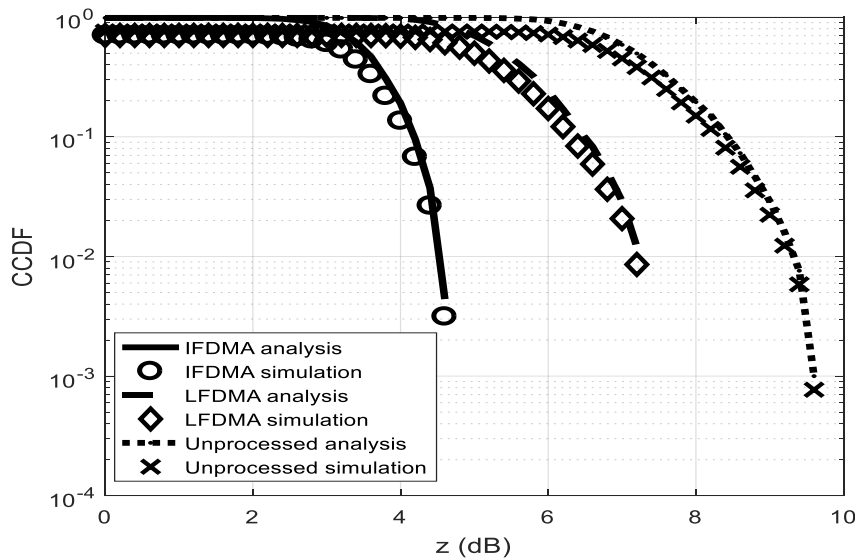


Figure 7: PAPR distribution of analytic and simulated OFDMA, IFDMA and LFDMA at CR = 1.2 with 64 QAM modulated symbols.

In Van Nee and De Wald (1998), linear minimum mean squared error (LMMSE) was proposed and adopted in this work. Then, the proposed algorithm was tested under doubly dispersive channel presented in (Chiavaccini

and Vitetta 2000) and compared with Shafter and Rao (2016) and Liu et al. (2018) in Figure 12. Both comparisons use 16 QAM modulation with fixed CR of 1.2. It is observed that the Liu et al (2018) method agrees with the proposed IFDMA except for

very small values of signal power where Liu et al. (2018) benefit from time diversity gain. In both cases, the proposed hybrid method proves to be superior over Shafter and Rao (2016) by at least 7 dB at error rate of 10^{-3} for the former and 3 dB at error rate of 10^{-1} for the latter. At higher signal power levels i.e., above 30 dB, both methods converge. This is

from the fact that the probability of symbol detection increases at higher signal power levels. The bit error rate (BER) performance is observed in Figure 13. The analytical BER performance uses derived equation 32 for the system operating under doubly dispersive channels with 16 QAM and CR of 1.2.

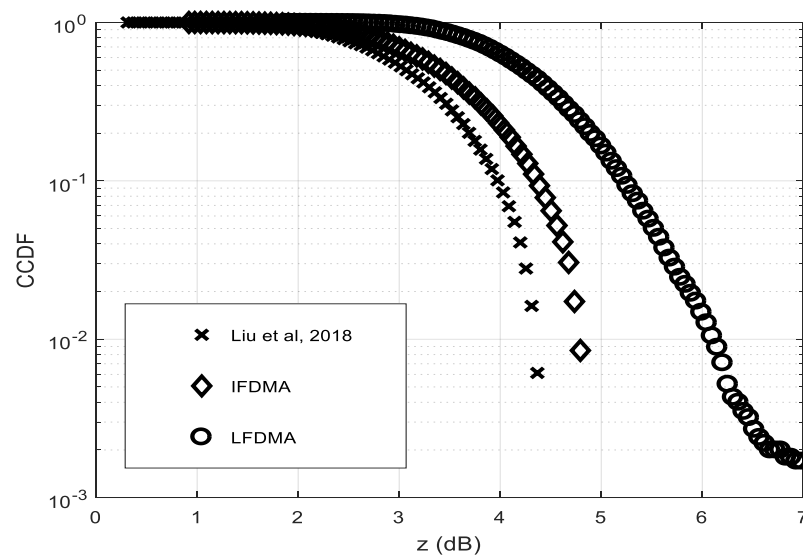


Figure 8: Comparison of PAPR distribution for Liu et al. (2018) and proposed algorithm with CR = 1.2 and 64-QAM

Comparisons of the analytical BER results for unprocessed and processed OFDM signal with computer simulations show very good agreement. The BER results are further compared with those presented in Liu et al. (2018) method. The close agreement confirms the accuracy of the analysis done in equations 29 to 32. It is well understood that the original OFDM signals have sharp power spectrum. This characteristic is sometimes affected by the PAPR reduction schemes. It is also noted that clipping technique can cause spectral regrowth of spectrum side lobes. These effects have been taken care by optimizing the

clipping ratio with the number of subcarriers used M , number of users' S and addition of the pulse shaping filter before transmission. The optimum clipping ratio is observed to be 1.2. The proposed algorithm is of low complexity, which is key in the implementation context. The existing trellis-assisted and MFTN have a disadvantage of being too complex to realize and consume more energy for matrices inversions when executed. Therefore, the proposed hybrid blind algorithm provides a practical alternative for PAPR reduction in systems employing OFDM technique.

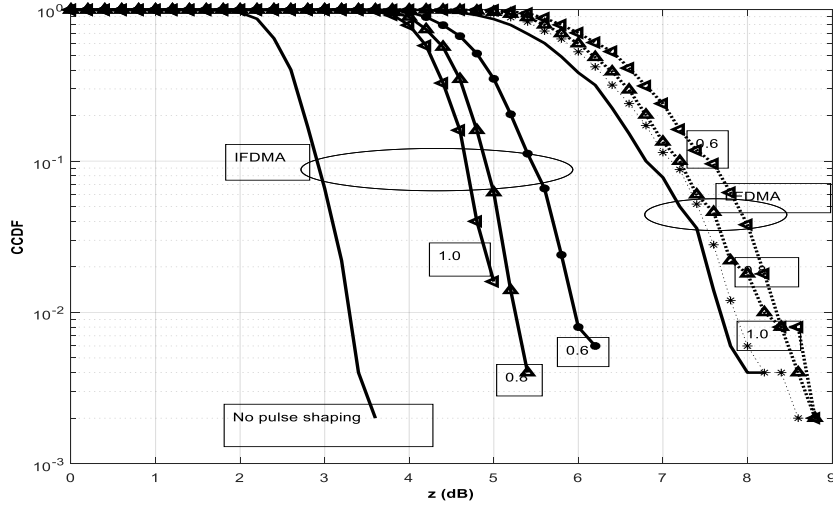


Figure 9: PAPR distribution of the proposed algorithm with pulse shaping.

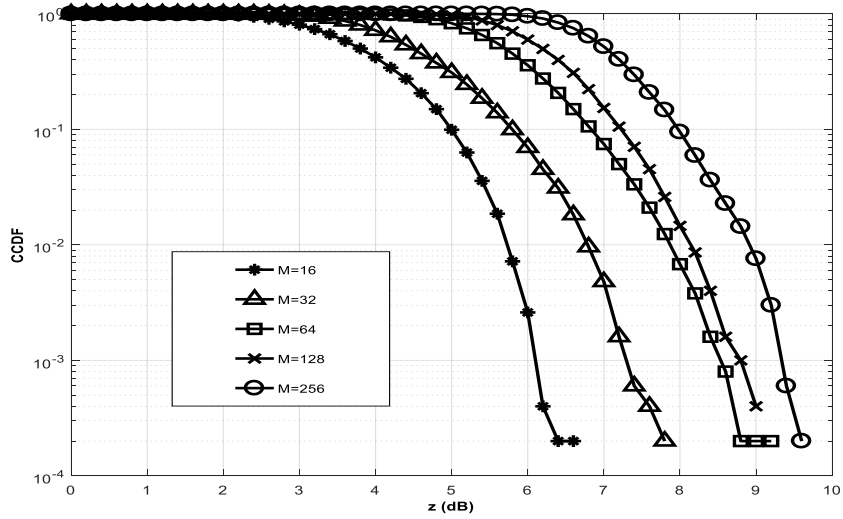


Figure 10: PAPR performance of the proposed algorithm with varying user block size M .

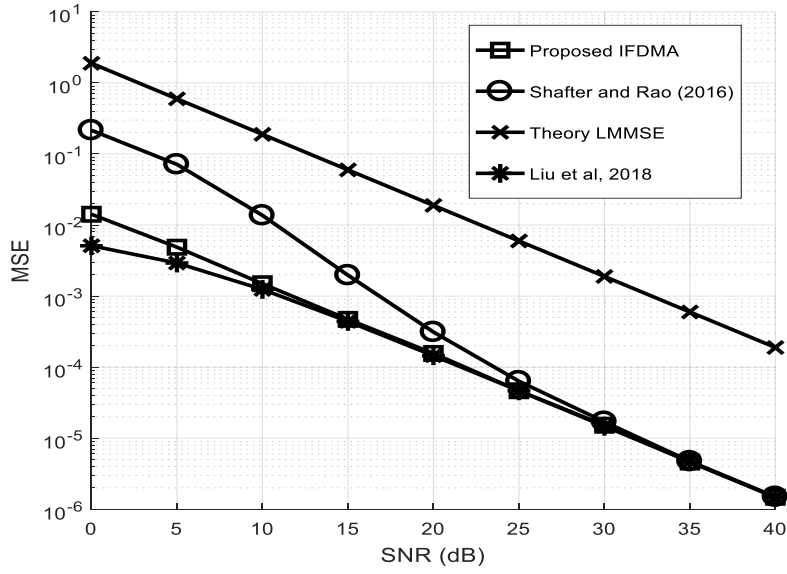


Figure 11: Performance of the proposed algorithm over AWGN channel.

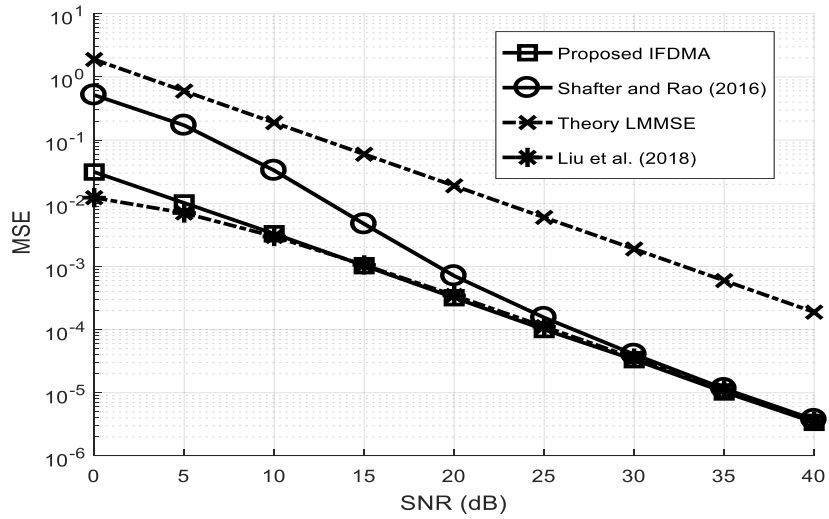


Figure 12: Performance of the proposed algorithm over doubly dispersive channel.

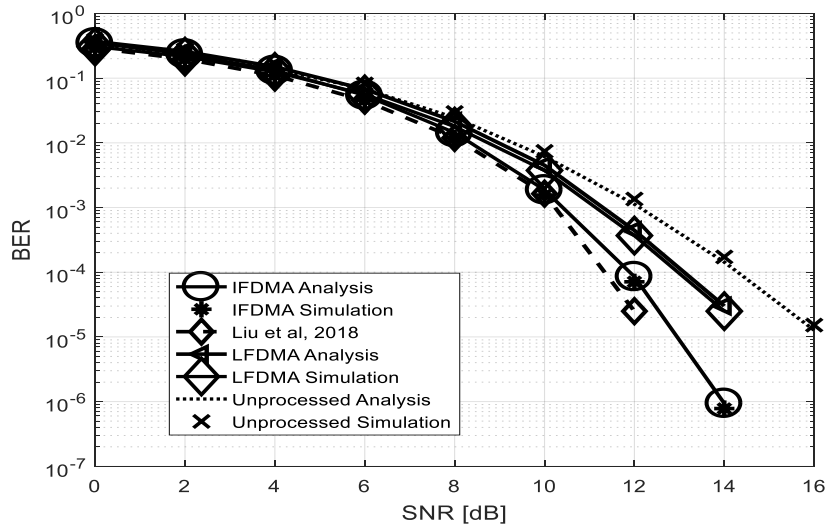


Figure 13: BER analytical and simulated performance of the proposed algorithm.

Conclusion

OFDM is a very attractive technique of choice for communications systems due to its channel robustness and better spectral efficiency. However, high PAPR in OFDM systems degrades energy efficiency leading to higher error rate performance. In this study hybrid blind PAPR reduction algorithm which is a combination of DFT spreading and clipping method, has been presented. The hybrid method has proven to be less complex with better performance, of more than 7 dB PAPR reduction at error rate 10^{-3} than the existing blind PAPR algorithms in flat fading channels. In doubly dispersive channels the improvement is 3 dB at error rate of 10^{-1} . The technique used, DFT-spreading, has been adopted for uplink transmission in 3GPP LTE (Release 8), which has evolved into one of the candidate radio interface technologies for the IMT-Advanced standards in ITU-R. The proposed hybrid method is an added advantage to the already existing standards in ITU-R. Future works should look on the channel characterization and signal

conditioning to maximize the energy efficiency of OFDM transmit signal.

References

Ann PP and Jose R 2016 Comparison of PAPR reduction techniques in OFDM systems. *Int. Conf. Comm. Electr. Sys.* 1: 1-5.

Cheng Y, Zhang J, Zhang Jun, Xiao M, Deng R and Chen L 2017 DFT-Spread combined with clipping method to reduce the PAPR in VLC-OFDM system. *IEEE Conf.* 1: 1462-1466.

Chiavaccini E and Vitetta GM 2000 Performance analysis of OFDM signaling over doubly selective fading channels. *IEEE Global Telecom. Conf.* 2: 975-979.

Cox C 2014 An Introduction to LTE, LTE-Advanced, SAE, VoLTE and 4G Mobile Communications. 2nd Ed, John Wiley and Sons.

Davis JA and Jedwab J 1997 Peak-to-mean power control and error correction for OFDM transmission using Golay sequences and Reed-Muller codes. *Electronic. Lett.* 33(4): 267-268.

- Fanggang W and Xiaodong W 2011 Coherent Optical DFT-Spread OFDM. *J. Adv. Optical Tech.* 11: 1-4.
- Han SH and Lee JH 2005 An overview of peak-to-average power ratio reduction techniques for multicarrier transmission. *IEEE J. Wireless Comm.* 12(2): 56-65.
- Ikpehai A, Adebasi B, Rabie KM, Fernando M and Wells A 2017 Energy-efficient vector OFDM PLC systems with dynamic peak-based threshold estimation. *IEEE J. Open Access* 5: 10723-10733.
- Joo HS, No JS and Shin DJ 2010 A blind SLM PAPR reduction scheme using cyclic shift in STBC MIMO-OFDM system. *Int. Conf. Information and Comm. Tech. Convergence*: 272-273.
- Li X and Cimini LJ 1998 Effects of clipping and filtering on the performance of OFDM. *IEEE Comm. Lett.* 2(20): 131-133.
- Litsyn S 2007 Peak Power Control in Multicarrier Communications, Cambridge University Press.
- Liu A, Peng S, Song L, Liang X, Wang KE and Zhang Q 2018 Peak-to-average ratio of multicarrier faster than nyquist signals: distribution, optimization and reduction. *IEEE J. Open Access* 6: 11977-11987.
- Mounir M, Youssef MI and Tarrad IF 2017 On the effectiveness of deliberate clipping PAPR reduction technique in OFDM systems. *IEEE conf. 1*: 21-24.
- Myung HG, Lim J and Goodman DJ 2006 Single carrier FDMA for uplink wireless transmission. *IEEE J. Vehicular Tech. Magazine* 1(3): 30-38.
- Offiong FB, Sinanović S and Popoola WO 2017 On PAPR reduction in pilot-assisted optical OFDM communication systems. *IEEE J. Open Access* 5: 8916-8929.
- Papoulis A and Pillai SU 2002 Probability, Random Variables and Stochastic Processes. 4th Ed, McGraw-Hill, New York.
- Proakis JG 2001 Digital communications. 4th Ed, McGraw-Hill, New York.
- Saeedi H, Sharif M, and Marvasti F 2002 Clipping noise cancellation in OFDM systems using oversampled signal reconstruction. *IEEE. Comm. Lett.* 6(2): 73-75.
- Shafter E and Rao RK 2016 CF technique with CPM mappers in OFDM systems for reduction of PAPR. *IEEE Canadian Conf. Electr. Computer Eng.* 1-5.
- Sriharsha MR, Dama S and Kuchi K 2017 A complete cell search and synchronization in LTE. *EURASIP J. Wireless Comm. Networking* 2017(1): 101.
- Thompson SC 2005 *Constant envelope OFDM phase modulation*, PhD thesis, University of California, San Diego, USA.
- Van Nee R and De-Wild A 1998 Reducing the peak-to-average power ratio of OFDM. *IEEE Vehicular Tech. Conf.* 3:2072-2076.
- Wang X, Tjhung TT, and Ng CS 1999 Reduction of peak-to-average power ratio of OFDM systems using a companding technique. *IEEE. Trans. Broadcast.* 45(3): 303-307.
- Yoshizawa R and Ochiai H 2017 Trellis-assisted constellation subset selection for PAPR reduction of OFDM signals. *IEEE Trans. Vehicular Tech.* 66(3): 2183-2198.